Published in final edited form as:
Cancer Res. 2013 March 15; 73(6): 1668–1675. doi:10.1158/0008-5472.CAN-12-3810.

Trp53 inactivation in the tumor microenvironment promotes tumor progression by expanding the immunosuppressive lymphoid-like stromal network

Gang Guo[1], **Luis Marrero**[2], **Paulo Rodriguez**[1,2], **Luis Del Valle**[1,3], **Augusto Ochoa**[1], and **Yan Cui**[1,2]

[1] Louisiana State University Medical Center, Stanley Scott Cancer Center New Orleans, LA 70112

[2] Department of Microbiology, Immunology, and Parasitology, Louisiana State University Medical Center, New Orleans, LA 70112

[3] Department of Pathology, Louisiana State University Medical Center, New Orleans, LA 70112

Abstract

Inactivation of the tumor suppressor *p53* through somatic mutations, observed in 50% of human cancers, is one of the leading causes of tumorigenesis. Clinical and experimental evidence also reveals that *p53* mutations sometimes occur in tumor-associated fibroblasts, which correlate with an increased rate of metastases and poor prognosis, suggesting that p53 dysfunction in the tumor microenvironment (TME) favors tumor establishment and progression. To understand the impact of *p53* inactivation in the TME in tumor progression, we compared the growth of subcutaneously inoculated B16F1 melanoma in $p53^{null}$ and WT mice. Interestingly, tumor growth in $p53^{null}$ mice was greatly accelerated, correlating with marked increases in $CD11b^{+}Gr\text{-}1^{+}$ myeloid-derived suppressor cells (MDSCs), $FoxP3^{+}$ regulatory T cells, and a loss of effector function, compared with those in WT mice. This augmented immunotolerant TME in $p53^{null}$ mice was associated with a marked expansion of a specialized stromal network in the tumor and spleen. These stromal cells expressed markers of fibroblastic reticular cells of lymphoid organs and were readily expanded in culture from $p53^{null}$, but not WT, mice. They produced high levels of inflammatory cytokines/chemokines and immunosuppressive molecules, thereby enhancing MDSC differentiation. Furthermore, they significantly accelerated tumor progression in WT mice when co-injected with B16F1. Together, our results demonstrate that tumor-stroma interaction in hosts with dysfunctional p53 exacerbates immunosuppression by expanding the lymphoid-like stromal network that enhances MDSC differentiation and tumor progression.

Keywords

p53 inactivation; tumor microenvironment; stroma; myeloid-derived suppressors; fibroblastic reticular cells

* Corresponding author: Louisiana State University Medical Center, New Orleans, LA 70112 Phone: 1-504-568-4636 Fax: 1-504-568-8500 ycui@lsuhsc.edu.

Conflict-of-interest: The authors disclose no conflicts of interest.

Introduction

The tumor suppressor p53 (Trp53, p53) inhibits tumorigenesis by inducing apoptosis and senescence of aberrant cells (1-3). *Trp53* somatic mutations, observed in about 50% of human cancers and some autoimmune pathological tissues, are major causes of tumorigenesis (1-4). Besides *p53* mutations, inactivation of the p53 pathway happens under various physiological and pathological conditions, including viral infection, oncogene activation, and aging (1-3). Furthermore, p53 inactivation also occurs in other components of the tumor microenvironment (TME), including cancer-associated fibroblasts (CAFs), which is associated with an increased rate of metastases and poor prognosis (5, 6). The TME, a complex cellular and molecular network of immune cells, stromal cells, extracellular matrix, and cytokines/chemokines, is crucial in immunomodulation that impacts tumor development, progression, and metastases (7-9). Studies by our laboratory and others showed that innate and adaptive immunities in $p53^{null}$ hosts are skewed towards pro-inflammation (10, 11). However, it is largely unexplored whether *p53* inactivation in the TME alters the immunological milieu, which exacerbates tumor progression.

Here, we hypothesized that *p53* inactivation in the TME favors tumor establishment and progression. By employing B16F1 melanoma, which maintains functional p53, we demonstrated that their growth in $p53^{null}$ mice upon subcutaneously (s.c.) inoculation was greatly accelerated, associated with an expansion of the lymphoid-like stromal network, compared with that in WT mice. The $p53^{null}$ stroma promoted tumor progression by expressing pro-inflammatory cytokines/chemokines, arginase I, and inducible nitric oxide synthase (iNOS) and by augmenting the accumulation of myeloid-derived suppressor cells (MDSCs).

Materials and Methods

Mice

$Trp53^{null}$ (B6.129S2-*Trp53*^{tm1tyj}/J) and *C57BL/6* mice, purchased from the Jackson Laboratories (Bar Harbor, ME), were maintained under specific pathogen-free conditions in the LSUHSC animal care facility following approved LSUHSC-IACUC protocols.

Tumor inoculation

B16F1, purchased from ATCC (Manassas, VA), was maintained in DMEM (Invitrogen, Carlsbad, CA) with 10% FBS and injected subcutaneously at 2×10^5/mouse. Tumors were measured every other day and calculated as: volume = (length × width) × (length + width)/2.

Histology and fluorescent immunohistochemistry (IHC)

H&E histology and IHC were performed following standard protocols and viewed by a licensed pathologist. Antibody dilutions for IHC were: ER-TR7 (5 μg/ml), Lyve-1 (5 μg/ml), α-smooth muscle actin (1 μg/ml, Abcam, Cambridge, MA), Gp38 (5 μg/ml), CD31 (5 μg/ml), CD11b (1 μg/ml, Biolegend, San Diego, CA), and Alexa Fluor-labeled secondary antibodies (2 μg/ml, Invitrogen). Vasculature and stroma quantification was performed using Slidebook software (Intelligent imaging Innovations, Denver, CO).

Flow cytometry

All antibodies were purchased from BD Biosciences (San Jose, CA) unless otherwise specified. Tumors were cut into 1 – 2 mm^3 pieces and digested with liberase (0.5 wU/ml, Roche, Switzerland) and DNase I (100 μg/ml, Sigma) in DMEM at 37°C for 30 min. MDSCs were enriched using EasySep® mouse CD11b positive selection kits (Stemcell Technologies, Canada). Regulatory T cells were analyzed as $CD4^+CD25^{hi}Foxp3^+$

(Ebioscience, San Diego, CA) cells. The effector cell function was determined via intracellular cytokine staining following standard protocols. FACS acquisition was performed using a FACSCalibur and analyzed using FlowJo (Tree Star Inc., Ashland, OR).

Splenic stromal cell (SPSC) isolation and expansion

Spleens, cut and digested with liberase and DNase I at 37ºC for 30 min, were subsequently cultured at 5×10^6/ml in DMEM with 10% FBS for 3 – 5 days. The $CD45^-$ population from adherent cells was enriched by depletion of $CD11b^+$-cells to >95% $CD45^-$ and was passaged twice a week. Their responses to B16F1-soluble factors were evaluated after a 6-hour exposure to B16F1conditioned medium (50%). Their effects on tumor growth were evaluated by injection of 1×10^5 SPSCs alone or mixed with 2×10^5 B16F1 s.c. to WT mice.

Real-time RT-PCR

Total RNA was harvested using Qiagen (Duesseldorf, Germany) RNeasy Kits. Reverse transcription was performed with 1 μg total RNA, followed by real-time PCR using PrimeTime® qPCR primers (Integrated DNA Technologies, IA) and a BioRad CFX96 (BioRad Life Science Research, Hercules, CA).

Bone marrow derived MDSCs

Bone marrow cells were cultured in DMEM containing 10% FBS, 100 ng/ml G-CSF, and 10 ng/ml IL-6 (PeproTech, NJ) at 1×10^6/ml with or without SPSCs for 4 days.

BrdU (5-bromodeoxyuridine) labeling

Tumor bearing mice were injected intraperitoneally with 1 mg of BrdU. $BrdU^+$ cells were analyzed via intracellular staining 24 h post-injection (BD Biosciences). Cultured BM-MDSCs were labeled with 10 μM BrdU for 2 h.

Multiplex cytokine assays

Mouse serum was analyzed using the Millipore (Billerica, MA) mouse Cytokine/ Chemokine-Premixed kit (MPXMCYTO70KPMX32) using Bio-Plex Manager (Bio-Rad Laboratories).

Statistical analysis

The differences between genotypes and/or treatments were analyzed via two-tailed Student's t-tests using SigmaPlot (Systat Software Inc.). Statistical significance was set at $p < 0.05$.

Results and Discussion

Trp53^{null} hosts augment tolerogenic tumor microenvironment and promote tumor progression

Previous studies suggest that *p53* inactivation enhances inflammation (10-12). To investigate whether *p53*^{null}-mediated inflammation promotes tumor progression, we compared B16F1 progression in WT and *p53*^{null} mice. As expected, B16F1 progressed more rapidly in *p53*^{null} mice (Fig. 1A), associated with significant alterations in tumor infiltrating leukocytes ($CD45^+$-TILs), - a 50% reduction in TIL-CD8 and a reciprocal increase in $CD11b^+$ myeloid cells, compared with those in WT mice (Fig. 1B). These were in agreement with IHC results (Fig. S1). Furthermore, IFN-γ- and IL-17A-producing effectors in *p53*^{null}–TILs were markedly suppressed despite a comparable percentage of TIL-CD4 and TNF-α producing cells between *p53*^{null} and WT mice (Fig. 1B - D). It is noteworthy that the

exacerbated immunotolerance in *p53*^{null} mice was more profound in the TME because the frequencies of effectors and Tregs in the spleen of WT and *p53*^{null} mice were comparable (Fig. S2). These results suggest that *p53* inactivation in hosts TME favors tumor progression by augmenting immunotolerance.

The accelerated tumor progression in *p53*^{null} hosts is associated with an enhanced MDSC accumulation and expansion of lymphoid-like stromal network within the TME

The CD11b^{+} population usually comprises heterogeneous myeloid cells, including CD11b^{+}Gr-1^{+} MDSCs, dendritic cells, granulocytes, and macrophages (13). Further analyses of B16F1-TILs CD11b^{+} cells in WT and *p53*^{null} mice showed that they were predominately MDSCs (TIL-MDSC) with comparable compositions of heterogeneous Ly6G^{hi}Ly6C$^{mod/lo}$ granulocytic (G)-MDSCs and Ly6G^{-}Ly6C^{hi} monocytic (M)-MDSCs (Fig. 2A and Fig. S3A). Nevertheless, the absolute number of TIL-M-MDSCs and total TIL-MDSCs in *p53*^{null} mice was significantly higher than that in WT mice (Fig. 2A). Functional analyses indicated that on a per cell basis, *p53*^{null} TIL-MDSC showed a similar capacity in suppressing the proliferation of activated T cells to WT TIL-MDSC (Fig. S3B), implying that the augmented immunosuppression in *p53*^{null} mice mainly results from their increased MDSC number. *In vivo* BrdU labeling of proliferating cells showed that BrdU^{+} TIL-MDSCs, but not TIL-CD11b^{+}Gr-1^{-} cells, almost doubled in tumor bearing *p53*^{null} mice compared with those in WT counterparts (Fig. 2B), suggesting that *p53* inactivation in the TME enhances the proliferation of MDSCs.

Recent studies suggest that MDSCs in the TME augment angiogenesis. Pathological examination of tumor specimens revealed that tumors growing in *p53*^{null}, but not WT, mice appeared to be organized into isle-like structures with marked increases in vasculatures (Fig. 2C). Emerging evidence suggests that during inflammation and tumor progression, lymphatic vasculatures and fibroblasts form a network reminiscent of the specialized stroma of secondary lymphoid organs (14, 15). Analyses of B16F1 tumors demonstrated marked increases in both blood endothelial cells (BEC, CD45^{-}CD31^{+}GP38^{-}Lyve-1^{-}) and lymphatic endothelial cells (LEC, CD45^{-} CD31^{+}GP38^{+}Lyve-1^{+}), associated with increased TIL-CD11b^{+} cel1ls in *p53*^{null} hosts (Fig. 2D). More strikingly, a fibroblast network, reminiscent of fibroblastic reticular cells (FRC) that are ER-TR7^{+}α-SMA^{+}(α-smooth muscle actin)GP38^{+} (15), was expanded extensively in tumors from *p53*^{null} mice compared with that from WT mice (Fig. 2D). These results suggest that *p53* inactivation in the TME provides a permissive environment for angiogenesis and expansion of FRC-like network.

B16F1 establishment in *p53*^{null} hosts promotes systemic increases in proinflammatory cytokines, MDSCs, and the stromal network in the spleen

To understand how *p53*^{null} TME encourages MDSC proliferation/accumulation, we first examined host cytokine milieu as it provides essential signals for MDSC development (13). In WT tumor bearing mice compared with non-tumor bearing mice, serum G-CSF and CXCL1 (KC) levels doubled and tripled, respectively (Fig. 3A). Likewise, serum G-CSF, CXCL1, and IL-6 in *p53*^{null} tumor bearing mice showed a 4 – 10 fold increases compared with non-tumor bearing mice (Fig. 3A). Further analysis of splenic MDSCs (SP-MDSC) in tumor bearing WT and *p53*^{null} mice showed that both M-MDSCs and G-MDSCs in the spleen of *p53*^{null} mice were significantly higher due to their marked increases in proliferation, i.e. BrdU^{+} SP-MDSCs (Fig. 3B&C). Further IHC analyses also confirmed a significant expansion of the FRC-network in the spleen of tumor bearing *p53*^{null} mice compared with non-tumor bearing *p53*^{null} mice and tumor bearing WT mice (Fig. 3D). Thus, our results suggest that tumor-stroma interaction in the TME lacking functional p53 promotes inflammation, accumulation of MDSCs, and expansion of the FRC-network.

Trp53^{null} splenic fibroblastic stroma enhances MDSC differentiation and markedly accelerates tumor progression in WT mice

Given the essential role of lymphoid FRC-network in immune regulation (15) and the role of SP stroma in inducing regulatory dendritic cells (16), we postulated that *p53*^{null} stroma augments MDSC development. Interestingly, splenic CD45^{-} stromal cells, termed SPSCs, from tumor bearing *p53*^{null}, but not WT, mice were readily expanded in culture. Further analyses showed that SPSCs, differing from mouse embryonic fibroblasts (MEF, Fig. S4), were CD106^{hi}CD54^{+}GP38^{+}Sca-1$^{lo/-}$ lymphoid FRC-like cells (Fig. 4A). To assess the function of SPSCs in promoting MDSC differentiation under a cytokine milieu mimicking B16F1 tumor bearing mice (Fig. 3A), we tested BM-MDSC differentiation in G-CSF + IL-6. Unlike G-CSF + GM-CSF (17), which predominantly induced M-MDSCs (Fig. S5), G-CSF + IL-6 supported the differentiation of heterogeneous M-MDSCs and G-MDSCs, resembling the composition of TIL-MDSCs (Fig. 2A&S3A). In the absence of SPSCs, comparable number of BM-MDSCs was derived from the BM of WT and *p53*^{null} cells (Fig. 4B). Strikingly, *p53*^{null} SPSCs enhanced BM-MDSC differentiation of WT and *p53*^{null} cells by 60% and 100%, respectively, mainly by enhancing their proliferation (Fig. 4B and Fig. S6).

Further analyses of the cytokine/chemokine profile of *p53*^{null} SPSCs via quantitative real-time RT-PCR showed that they expressed higher levels of proinflammatory cytokines/chemokines and immunosuppressive mediators, including IL-6, IL-10, CCL3, CCL21, Arg1, and iNOS, compared with *p53*^{null} MEF (Fig. 4C). Moreover, exposure of SPSCs to B16F1 conditioned medium further enhanced the expression of CXCL12, CCL3, and IL-10 (Fig. 4C). To confirm that *p53*^{null} stroma hastens tumor progression, we injected *p53*^{null} SPSCs either alone or mixed with B16F1 to WT mice and showed that co-injection of SPSCs with B16F1 substantially accelerated tumor growth as early as day 8 post-injection (Fig. 4D). These results strongly suggest that the lymphoid-like stroma in *p53*^{null} hosts is immunosuppressive and that tumor-stroma interaction exacerbates immunosuppression, augments MDSC development, and accelerates tumor progression.

Taken together, this study demonstrates that *p53* inactivation in the TME promotes immunosuppression and tumor progression by expanding the lymphoid-like stromal network. The crucial role of the TME in tumor initiation and progression has been increasingly appreciated (7-9, 13). However, the immunological consequence of *p53* inactivation in the TME involving tumor-stroma interaction has been unexplored. Early studies suggest that *p53* inactivation in CAFs enhances tumor progression via paracrine effects of CXCL12 (18). Our observed high level CXCL12 expression in *p53*^{null} SPSCs agrees with this notion. More importantly, our results further demonstrate that the *p53*^{null} lymphoid-like stromal network skews the TME towards pro-inflammation via various inflammatory cytokines/chemokines and immunosuppressive molecules. Specifically, we postulate that the elevated G-CSF, IL-6, and IL-10 in circulation and/or the TME of *p53*^{null} hosts provide crucial differentiation and survival signals for MDSCs and Tregs, respectively, while the increased expression of CXCL1, CCL3, and CCL21 plays a vital role in recruiting the immunosuppressive populations to the TME (9, 13, 19, 20). Additionally, iNOS and Arg1 in the TME further augment the function of those immunosuppressors (9, 13). CXCL1, produced by melanomas or stroma, is a pro-tumor chemokine either directly stimulates tumor via paracrine effect or indirectly via pro-inflammation-mediated recruitment of MDSCs (19, 20). Indeed, we detected a low level expression of CXCL1 in B16F1, which is further enhanced by tumor-stroma or tumor-immune cell interaction in the *p53*^{null} TME. Therefore, the strong immunosuppressive and pro-tumor microenvironment in *p53*^{null} hosts is likely a result of concerted multi-dimensional interactions involving tumor, stroma, and immune cells.

The *p53*^{null} mice used in this study best resemble those individuals with Li-Fraumeni syndrome (2). However, the immunological mechanism revealed in this study by which *p53* inactivation/dysfunction in the TME enhances tumor progression should have broad clinical implications because *p53* inactivation occurs frequently during physiological and pathological processes via various mechanisms, including the activation of oncogenes and viral proteins, in addition to somatic mutations (1-3, 5, 6).

In summary, this is the first study that elucidates the underlying mechanism by which *p53* inactivation immunomodulates the TME. These results underscore the importance and function of p53 in maintaining proper immunological microenvironment to suppress tumorigenesis and provide valuable information for novel therapeutics by targeting p53 activity in the stroma/TME.

Supplementary Material

Refer to Web version on PubMed Central for supplementary material.

Acknowledgments

We thank Drs. Tomoo Iwakuma, Daitoku Sakamuro, Suresh Alahari, Krzysztof Reiss, and Wanguo Liu for critical discussions.

Financial support: Supported by LCRC and NIH grants CA112065 to YC and P20RR021970 to AO.

References

1. Riley T, Sontag E, Chen P, Levine A. Transcriptional control of human p53-regulated genes. Nat Rev Mol Cell Biol. 2008; 9:402–412. [PubMed: 18431400]
2. Vousden KH, Lane DP. p53 in health and disease. Nat Rev Mol Cell Biol. 2007; 8:275–283. [PubMed: 17380161]
3. Soussi T. p53 alterations in human cancer: more questions than answers. Oncogene. 2007; 26:2145–2156. [PubMed: 17401423]
4. Yamanishi Y, Boyle DL, Rosengren S, Green DR, Zvaifler NJ, Firestein GS. Regional analysis of p53 mutations in rheumatoid arthritis synovium. Proc Natl Acad Sci U S A. 2002; 99:10025–10030. [PubMed: 12119414]
5. Hill R, Song Y, Cardiff RD, Van Dyke T. Selective evolution of stromal mesenchyme with p53 loss in response to epithelial tumorigenesis. Cell. 2005; 123:1001–1011. [PubMed: 16360031]
6. Patocs A, Zhang L, Xu Y, Weber F, Caldes T, Mutter GL, et al. Breast-cancer stromal cells with TP53 mutations and nodal metastases. N Engl J Med. 2007; 357:2543–2551. [PubMed: 18094375]
7. Kerkar SP, Restifo NP. Cellular constituents of immune escape within the tumor microenvironment. Cancer Res. 2012; 72:3125–3130. [PubMed: 22721837]
8. Swartz MA, Iida N, Roberts EW, Sangaletti S, Wong MH, Yull FE, et al. Tumor microenvironment complexity: emerging roles in cancer therapy. Cancer Res. 2012; 72:2473–2480. [PubMed: 22414581]
9. Ostrand-Rosenberg S, Sinha P. Myeloid-derived suppressor cells: linking inflammation and cancer. J Immunol. 2009; 182:4499–4506. [PubMed: 19342621]
10. Zhang S, Zheng M, Kibe R, Huang Y, Marrero L, Warren S, et al. Trp53 negatively regulates autoimmunity via the STAT3-Th17 axis. Faseb J. 2011; 25:2387–2398. [PubMed: 21471252]
11. Zheng SJ, Lamhamedi-Cherradi SE, Wang P, Xu L, Chen YH. Tumor suppressor p53 inhibits autoimmune inflammation and macrophage function. Diabetes. 2005; 54:1423–1428. [PubMed: 15855329]
12. Schetter AJ, Heegaard NH, Harris CC. Inflammation and cancer: interweaving microRNA, free radical, cytokine and p53 pathways. Carcinogenesis. 2010; 31:37–49. [PubMed: 19955394]

13. Gabrilovich DI, Ostrand-Rosenberg S, Bronte V. Coordinated regulation of myeloid cells by tumours. Nat Rev Immunol. 2012; 12:253–268. [PubMed: 22437938]

14. Shields JD, Kourtis IC, Tomei AA, Roberts JM, Swartz MA. Induction of lymphoidlike stroma and immune escape by tumors that express the chemokine CCL21. Science. 2010; 328:749–752. [PubMed: 20339029]

15. Turley SJ, Fletcher AL, Elpek KG. The stromal and haematopoietic antigen-presenting cells that reside in secondary lymphoid organs. Nat Rev Immunol. 2010; 10:813–825. [PubMed: 21088682]

16. Zhang M, Tang H, Guo Z, An H, Zhu X, Song W, et al. Splenic stroma drives mature dendritic cells to differentiate into regulatory dendritic cells. Nat Immunol. 2004; 5:1124–1133. [PubMed: 15475957]

17. Marigo I, Bosio E, Solito S, Mesa C, Fernandez A, Dolcetti L, et al. Tumor-induced tolerance and immune suppression depend on the C/EBPbeta transcription factor. Immunity. 2010; 32:790–802. [PubMed: 20605485]

18. Orimo A, Gupta PB, Sgroi DC, Arenzana-Seisdedos F, Delaunay T, Naeem R, et al. Stromal fibroblasts present in invasive human breast carcinomas promote tumor growth and angiogenesis through elevated SDF-1/CXCL12 secretion. Cell. 2005; 121:335–348. [PubMed: 15882617]

19. Dhawan P, Richmond A. Role of CXCL1 in tumorigenesis of melanoma. J Leukoc Biol. 2002; 72:9–18. [PubMed: 12101257]

20. Hembruff SL, Cheng N. Chemokine signaling in cancer: Implications on the tumor microenvironment and therapeutic targeting. Cancer Ther. 2009; 7:254–267. [PubMed: 20651940]

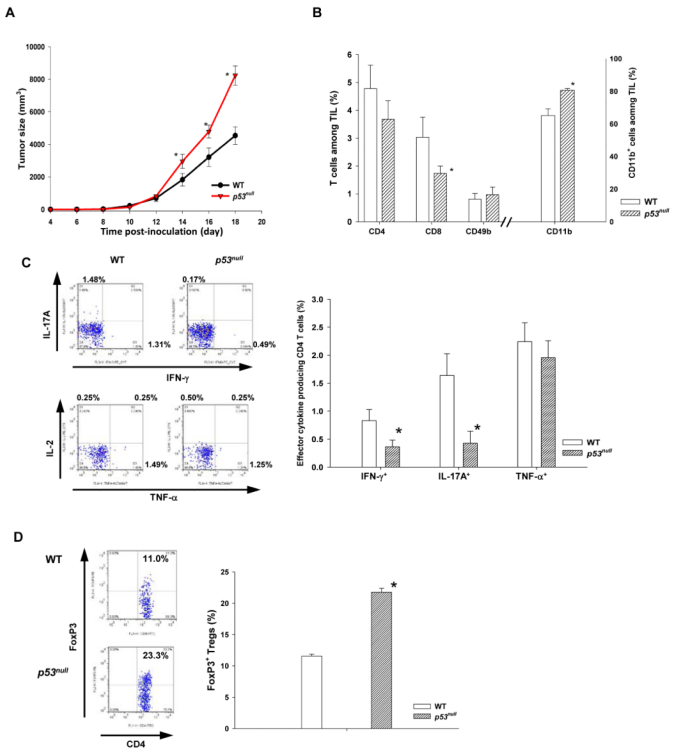

Fig. 1. *Trp53*^{null} hosts augment tolerogenic tumor microenvironment and promote tumor progression

WT and *p53*^{null} *C57/B6* mice were inoculated subcutaneously with 2 × 10^5 B16F1 cells. (A) Tumor size was measured every other day (n=10 - 15). (B) Mice were euthanized on day18 post-inoculation. CD4$^+$, CD8$^+$, CD49b$^+$, and CD11b$^+$ cells among tumor infiltrating leukocytes (TIL, CD45$^+$) were examined. (C) The percentage of effector cytokine producing TIL-CD4 and (D) FoxP3$^+$ regulatory T cells was determined. Results are presented as mean ± standard error (s.e.) of 5 – 10 mice from at least three independent experiments. * represents a significant difference ($p < 0.05$). Two-tailed Student's t-test.

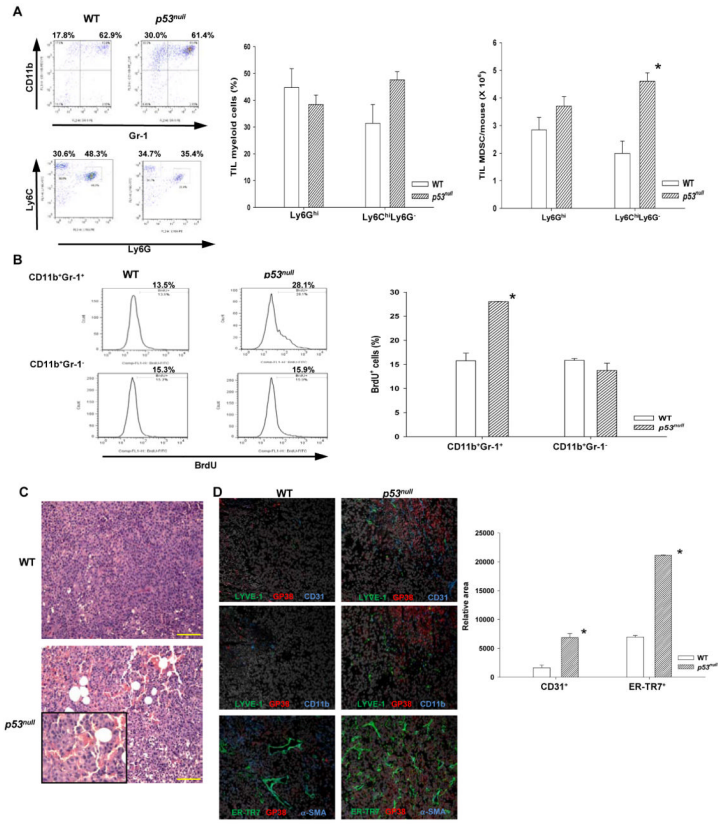

Fig. 2. The accelerated tumor progression in *p53*^{null} hosts is associated with an increase in MDSCs and expansion of lymphoid-like stromal network

(A) TIL-MDSCs and subpopulations from WT and *p53*^{null} mice were analyzed (n= 5-10). (B) Proliferating TIL-MDSCs in tumor bearing mice were analyzed as BrdU^{+}CD11b^{+}Gr-1^{+} cells 24 hours post-BrdU injection. (C) Representative tumor histology images from WT and *p53*^{null} mice. Scale bar = 100 mm. (D) Representative tumor IHC images (200X) from WT and *p53*^{null} mice revealing blood endothelial cells (BEC, LYVE-1^{-}Gp38^{-}CD31^{+}), lymphatic endothelial cells (LEC, LYVE-1^{+}Gp38^{+}CD31^{+}), fibroblastic reticular cells (FRC, ER-TR7^{+}Gp38^{+}α-SMA^{+}), and CD11b^{+} cells. The relative area of CD31^{+} vasculatures and ER-TR7^{+} FRC-stroma was determined using a computer-assisted program. Data are mean ± s.e. (n= 3). * denotes a significant difference ($p < 0.05$).

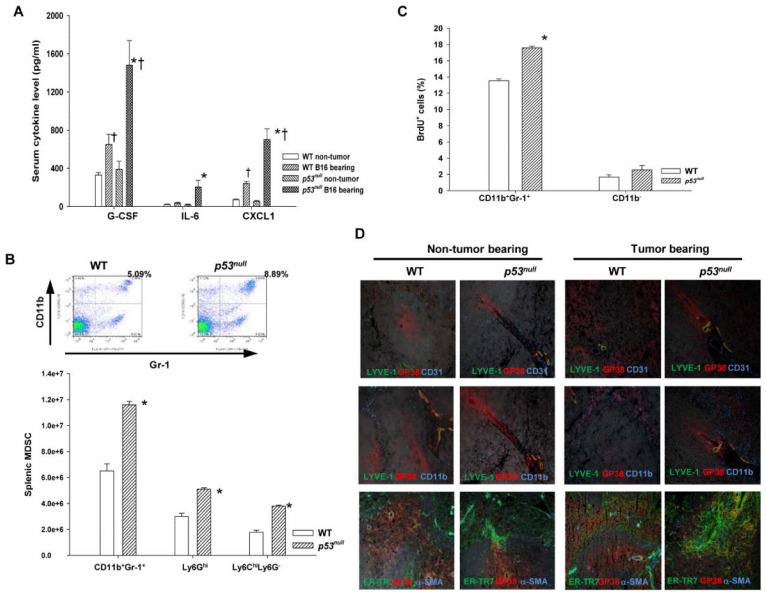

Fig. 3. B16F1 establishment in *p53*^{null} hosts promotes a systemic increase in proinflammatory cytokines, MDSCs, and stromal-network in the spleen

(A) Serum proinflammatory cytokines/chemokines in tumor bearing mice were determined via cytokine multiplex array (n=6). (B) The splenic MDSCs in tumor bearing WT and *p53*^{null} mice were analyzed. (C) Proliferating splenic MDSCs in tumor bearing mice were examined 24 hours post-BrdU injection. (n=3). (D) Representative splenic IHC images (200X) of non-tumor and tumor bearing mice. * denotes a significant difference ($p < 0.05$) between WT and *p53*^{null} mice under the same treatment, whereas † indicates a significant difference between non-tumor and tumor bearing mice.

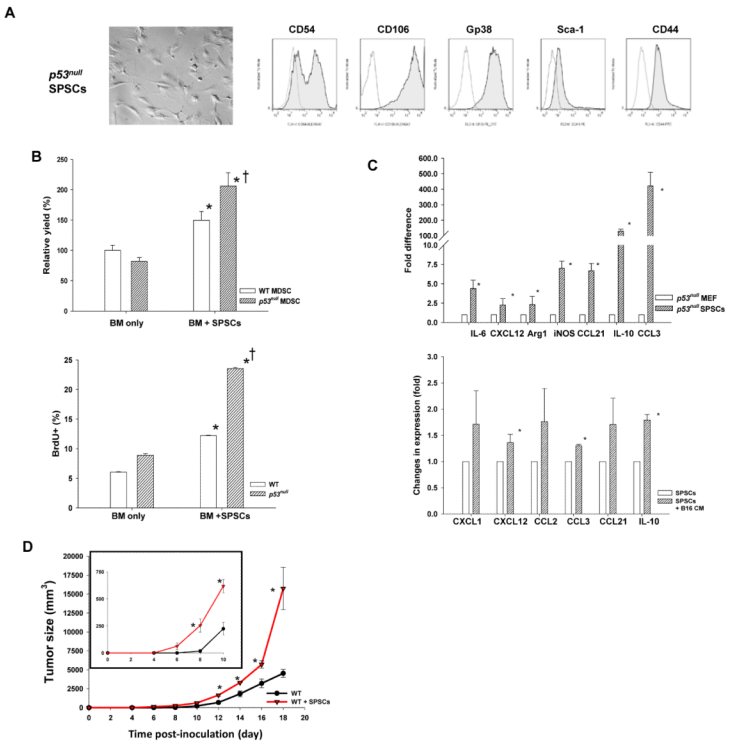

Fig. 4. *Trp53*^{null} splenic fibroblastic stroma enhances MDSC differentiation and accelerates tumor progression in WT mice

(A) A representative image (400X) and phenotypic analyses of CD45^{-} splenic stromal cells (SPSC) from tumor bearing *p53*^{null} mice. Open lines indicate isotype controls. (B) BM-MDSCs were differentiated in a 4-day culture with G-CSF and IL-6 with or without SPSCs. Their relative efficiency was normalized against that of WT BM-MDSCs without SPSCs, which was set as 100%. Proliferating (BrdU^{+}) BM-MDSCs were examined o day 4 (n=3). * denotes a significant difference ($p < 0.05$) between groups with and without SPSCs, whereas † indicates a significant difference between WT and *p53*^{null} BM-MDSCs. (C) Proinflammatory molecule expression in *p53*^{null} SPSCs compared with those in MEF, as well as their alterations upon a 6-hour exposure to B16F1-conditioned medium, was determined via real-time RT-PCR (n=3-5). (D) The tumor size in WT mice received 2×10^5 B16F1 or 2×10^5 B16F1 admixed with 1×10^5 *p53*^{null} SPSCs was compared (n=5). * denotes a significant difference ($p < 0.05$).